

PREPARATION, CHARACTERIZATION AND PHENOL ADSORPTION OF *Mangifera kemanga* Blume SEED

Siti Hadiati Mardiah¹⁾, Dian Arrisujaya^{1)*}, Devy Susanty¹⁾ and Nia Yuliani²⁾

¹⁾Department of Chemistry, Universitas Nusa Bangsa,

²⁾Department of Biology, Universitas Nusa Bangsa,

Jl. K.H. Sholeh Iskandar Km. 4 Cimanggu Tanah Sareal, Bogor 16166, Indonesia

ARTICLE INFO

Article history:

Received 13 Mei 2022,

Revised 02 Jul 2022,

Accepted 03 Jul 2022,

Available online 30 Jul 2022

Keywords:

- ✓ adsorption,
- ✓ Bogor,
- ✓ endemic,
- ✓ *Mangifera kemanga*,
- ✓ phenol

*corresponding author:

arrisujaya@unb.ac.id

<https://doi.org/10.31938/jsn.v12i3.410>

ABSTRACT

The potential of Mangifera kemanga Blume., an inexpensive biosorbent, for removing of hazardous substances such as phenols from its aqueous solution has been studied. The authors used Scanning Electron Microscope (SEM), Fourier Transform Infrared (FTIR) Spectrometers, and quantification to study the morphology and characterization of Mangifera kemanga Blume. seeds (MKS) biomass, as well as batch experiments to determine the percentage of phenol removed when pH, contact period, biosorbent dosage, and phenol concentration were varied. The Langmuir, Freundlich, Temkin, and Dubinin–Radushkevich isotherm models had been used to interpret the experimental results. The optimal values found in our research correspond to a pH of 6 for an MKS dosage of 35 g/L and a contact time of 45 minutes for initial phenol concentrations ranging from 5 to 25 mg/L. The result indicated that MKS was a particularly successful adsorbent for phenol chemisorption from aqueous solution.

INTRODUCTION

Hazardous and toxic substances are materials that can pollute or damage the environment, human health, and the survival of other living creatures directly or indirectly, contained in Indonesia's Minister of Environment's Regulation No. 5 of 2014. Hazardous wastewater created as a result of rapid industrial growth contributes significantly to environmental pollution (Haddow et al., 2014; Sharma et al., 2019). For example, phenol was detected in the wastewater of many manufacturing industries and must be managed properly because it is recognized as a priority pollutant from the US Environmental Protection Agency (EPA) (Ramírez-García et al., 2019; Sadh et al., 2018). The World Health Organization (WHO) allows a standard level of 0.001 mg/L for potable water quality (Mandal et al., 2019).

Several technologies for removing phenol and its derivatives have been investigated such as flocculation, ion exchange, membrane separation, solvent extraction, photodegradation, oxidation,

precipitation and adsorption (Khraisheh et al., 2020; Ponnuchamy et al., 2020). However, in the wastewater treatment industry, the adsorption technique is very common. Adsorption with various natural adsorbents is likely to be the most efficient and cost-effective treatment option for phenol removal (Arrisujaya et al., 2019; Zein, Hidayat, et al., 2014). Some of the essential requirements for selecting the best adsorbents are structural characteristics, adsorption capacity, the surface area, pore sizes, simple regeneration and numerous uses (Hevira et al., 2020; Moyo et al., 2017).

Many researchers were on the lookout for natural adsorbents that were both inexpensive and readily accessible, i.e. sugar palm fruit shell (Zein, Arrisujaya, et al., 2014), sandbox tree seed (Adewuyi et al., 2015), mango seed (Moyo et al., 2017) and its leaf (Khan et al., 2019), natural guava leaf (Ponnuchamy et al., 2020), rice husk ash (Mandal et al., 2019), velvet apple seed (Arrisujaya et al., 2019), almond shell (Hevira et al., 2020), etc. Some natural adsorbents contained



hydroxyl, carboxyl, amino, phosphate, and other functional groups that could act as phenol binding sites (Arrisujaya et al., 2019; Khan et al., 2019).

Mangifera kemanga Blume., the Bogor regency's identification flora, is a plant in the Anacardiaceae family (Sancoyo, 2018). This fruit seed is an affordable agricultural waste source for adsorbent. Here to state of the art, no research on the comprehensive characterization of *Mangifera kemanga* Blume. seed (MKS) had been published in the literature up to this time. The average content of MKS was almost similar to that of mango seeds, with carbs (69.22-79.78 %), fat (8.35-16.13 %), protein (5.6-9.5 %), starch (92 %), fiber (0.14-2.95 %), and ash (0.35-3.66 %), and these seeds also contained high content in tannins (Legesse & Emire, 2012). Furthermore, there was no confirmation of an authenticated sorption phenomenon for phenol removal based on mechanistic explanation using MKS from its natural state.

According to the authors' exhaustive quest, MKS had never been established for use in the bioreduced and environmentally safe adsorption of phenol. The suitability of the MKS adsorbent for phenol adsorption was investigated in this study. The equilibrium data of the adsorption process was then examined in order to improve comprehension of the adsorption process.

MATERIALS AND METHODS

Materials and Apparatus

The materials and chemicals used were *Mangifera kemanga* Blume. seed, nitric acid (HNO₃), sulfuric acid (H₂SO₄), hydrochloric acid (HCl), sodium hydroxide (NaOH), benzene, ethanol and phenol. All chemicals were purchased from Merck and were of pro analytical grade.

The following apparatus was used: UV-Vis Spectrophotometer (Optizen POP, Mecasys, Korea), Fourier Transform Infrared (FT-IR) Spectrometer (Alpha II, Bruker, USA) Scanning Electron Microscope (SEM) (JEOL JSM-6360LA, JEOL Ltd., Japan), in combination with an Energy Dispersive Spectrometer (EDS) (JEOL JED-2300T, JEOL Ltd., Japan).

Methods

Preparation of Biomass and Constituent Analysis

Kemang (*Mangifera kemanga* Blume.) fruits were collected from Bogor Regency's traditional market in Indonesia. The seeds were properly

cleansed with water in order to exclude any dust or adhering particles, then it was kept in the sun to dry. The cleaned seeds were pulverized and sieved using a mesh sieve with a mesh size of 100.

The constituents of *Mangifera kemanga* Blume. seed (MKS) biomass were analyzed using the methodology (Khan et al., 2019) described below.

Ash Content

In a porcelain crucible, 0.3 g of MKS biomass was dried in a hot air oven before becoming incinerated for 8 hours in a furnace of 700 °C. The ash percentage was determined by calculating the weight of cooled ash and following equation (1).

$$\text{Ash}(\%) = \frac{\text{weight of ash}}{\text{weight of biomass}} \quad (1)$$

Analysis of Extractives

3.0 g of MKS biomass (G₀) was agitated at 120 rpm in a flask containing benzene and ethanol solution (2:1) for 3 h at 30°C. The precipitate was dried in an oven (105–110 °C) and chilled before being weighed at a constant total mass (G₁). The extractive percentage was determined using an equation (2).

$$W_1(\text{Wt. } \%) = \frac{G_0 - G_1}{G_0} \times 100 \quad (2)$$

Hemicellulose Determination

The G₁ residue was refluxed for 3.5 hours following the analysis of extractive with 150 mL of 20 g/L NaOH solution. After that, the processed residue was cleaned, dried, and reweighed (G₂, g). The equation (3) was used to calculate the hemicellulose content.

$$W_2(\text{Wt. } \%) = \frac{G_1 - G_2}{G_0} \times 100 \quad (3)$$

$$W_3(\text{Wt. } \%) = \frac{G_4 - (1 - W_1)}{G_3} \times 100 \quad (4)$$

Lignin Determination

In a flask, 1.0 g of G₁ residue was dried in an oven to a constant total mass (G₃, g). The flask was filled with 30 mL H₂SO₄ and maintained at 15 °C for 24 h. Before being refluxed for an hour, the samples were washed with 300 mL of double-distilled water. Then, the chilled mixture was

rinsed three times with the double distilled, dried with in oven, and weighed. (G_4 , g). The determination of lignin percentage was described in equation (4).

Cellulose Determination

The cellulose content was determined using equation (5).

$$W_4(\text{Wt. \%}) = 100 - (W_1 + W_2 + W_3 + \text{Ash}) \quad (5)$$

Preparation of Biosorbent

MKS biomass was activated in 0.1 M HNO_3 solution for 2 hours, stirring occasionally, before being filtered. The wet material was then rinsed with distilled water to achieve a pH of neutral, before being filtered and dried. The acid-activated MKS prepared in this manner was used as a biosorbent (Arrisujaya, 2014).

Biosorption experiments – batch studies

The studies were carried out to see how effective the acid-activated MKS was at removing phenol from its aqueous solution. The experiments were conducted with process variables such as initial phenol concentration, pH, contact time, etc. In 100 mL closed flasks containing, aqueous phenol solution (50 mL) was poured (Arrisujaya et al., 2019; Nazaruddin et al., 2014). Dilution was accomplished by adding distilled water to produce the required concentrations of 5, 10, 15, 20, and 25 mg/L. The pH was changed from 2, 4, 6 and 8 by using HCl and NaOH. The required amount of MKS biosorbent (30 to 50 g/L) was mixed, and the solution was shaken in the electrically thermostatic shaker for 15 to 240 minutes. Finally, the residue was filtered out, and the filtrate's residual phenol concentration was determined using spectrometry method. All samples had absorbance measurements taken at 238 nm.

The percentage of phenol removal was calculated using equation (6).

$$E(\%) = \frac{C_o - C_e}{C_o} \times 100\% \quad (6)$$

where C_o and C_e (mg/L) are initial and equilibrium phenol concentrations, respectively.

Equation (7) was used to compute the amount of phenol adsorbed per unit biosorbent, q_e (mg/g) as follows:

$$q_e = \frac{C_o - C_e}{m} \times V \quad (7)$$

where V is the volume of the phenol solution in litres and m is the mass of MKS biosorbent in grams.

RESULTS AND DISCUSSION

MKS Biomass Analysis

The quantitative examination of MKS biomass components, as shown in Table 1, revealed that cellulose was the primary component of MKS, with lignin and hemicellulose serving as secondary and tertiary components, respectively.

Table 1. Components analysis of MKS biomass

Component	Wt(%)*
Ash	1.99 ± 0.20
Extractives	0.75 ± 0.01
Hemicellulose	18.68 ± 0.16
Lignin	24.95 ± 0.01
Cellulose	53.63 ± 0.01

* Dry weight percentage

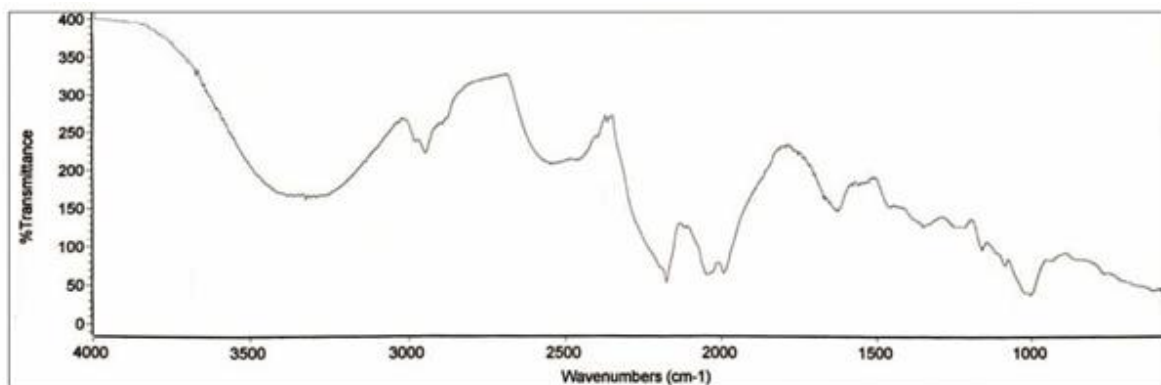


Figure 1. FTIR spectra of MKS biomass

Instrumental Characterization of MKS Biomass

Using potassium bromide (KBr) disks, Fourier transform infrared spectroscopy (FTIR) was utilized to assess the presence of surface functional groups on MKS biomass. The result of the functional groups determination of MKS biomass is shown in Figure 1. The FTIR spectrum of MKS biomass in Figure 1 revealed broadband near $3200 - 3600 \text{ cm}^{-1}$ and revealed the stretching frequency of O-H, C-H stretching at $2800 - 3000 \text{ cm}^{-1}$ (Hevira et al., 2020). The peaks at $1400 - 1600 \text{ cm}^{-1}$ were caused by the stretching frequency of aromatic C=C (Moyo et al., 2017). The presence of C-H bending and C-O stretching was indicated by the peak around $1080 - 1300 \text{ cm}^{-1}$, whereas the peaks at $1050 - 1150 \text{ cm}^{-1}$ indicated strong presence of C-O and C-O-C stretching.

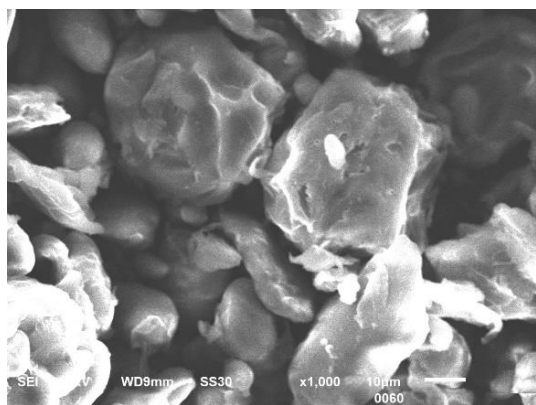


Figure 2. SEM topography of MKS biomass

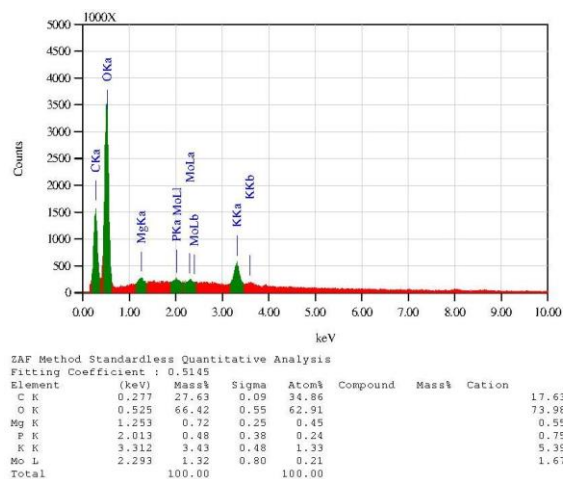


Figure 3. EDS spectra of MKS biomass

Scanning electron microscopy (SEM) in combination with an energy dispersive spectroscopy (EDS) analysis was carried out to analyze morphological traits and obtain elemental

characterization of biomass. Results of the MKS biomass SEM at 1000X magnification is shown in Figure 2. The result showed that MKS biomass has a rough, porous and variable surface over a vast region (Khan et al., 2019). The EDS spectra of MKS biomass revealed considerable indications of numerous elements (viz. C, O, Mg, P, K, and Mo) as a result of X-ray emissions of MKS powder surface macromolecules. (see Figure 3.).

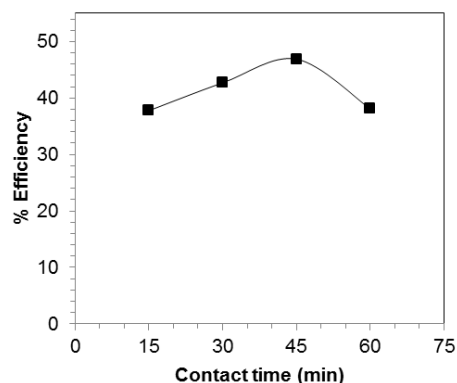


Figure 4. Efficiency percentage of phenol removal versus contact time

The Effect of Process Parameters on Phenol Removal by MKS

Effect of contact time

Therefore, the experiment was carried out throughout a range of contact times (15-240 minutes) with a constant initial phenol concentration of 10 mg/L, a fixed pH of 5.5, and a constant biosorbent dosage of 20 g/L. Figure 4 depicts a plot of percentage phenol removal with adsorption time that shows that the efficiency was initially moderate and then reached an equilibrium of 46.90 % at 45 minutes.

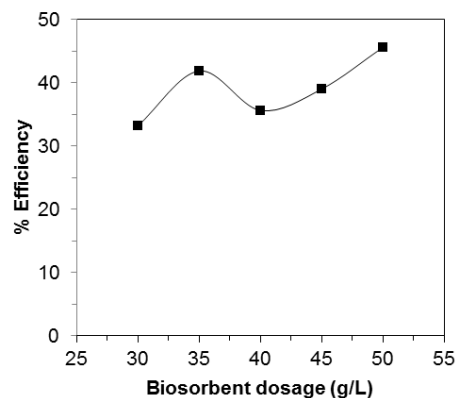


Figure 5. Efficiency percentage of phenol removal versus biosorbent dosage

The faster adsorption at first may be owing to a propensity to reach equilibrium after a specific period of time as a result of three mass transfer processes occurring in rapid succession (Hameed & Rahman, 2008). The first was film diffusion, in which the solute was dissolved as it passed through the solution. Pore diffusion was the second process, in which the solute migrated from the surface to the inside upon being adsorbed (Mandal et al., 2019).

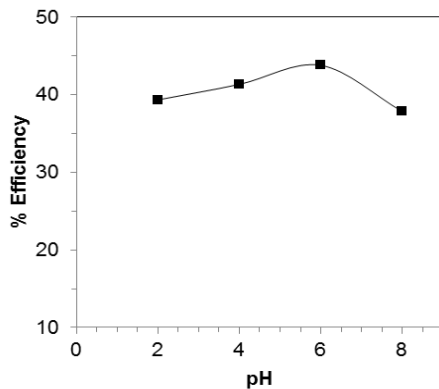


Figure 6. The percentage of phenol removal efficiency versus biosorbent pH

Effect of biosorbent dosage

The experiment was carried out with varying biosorbent dosage (30-50 g/L) with a constant initial phenol concentration of 10 mg/L, a fixed pH of 5.5, and at optimum contact time of 45 min. As the MKS dosage was increased, the efficiency percentage of phenol removal increased (Figure 5.), this could be explained by a rise in the amount of unoccupied sites on MKS, which could be used to occupy the readily accessible phenol (Khan et

al., 2019). Furthermore, the agglomeration of active sites might account for the differential adsorption behavior, resulting in a slight increase in adsorption percentage followed by a decrease (35 g/L) in phenol removal.

Effect of pH

The pH was thought to be an important factor because it affected the adsorption value (Zein, Arrisujaya, et al., 2014). The studies was carried out with different pH levels (2, 4, 6 and 8) with an initial phenol concentration of 10 mg/L as a fixed value, at optimum biosorbent dosage of 35 g/L, and at optimum contact time of 45 min. Figure 6 shows that the phenol removal effectiveness percentage was highest at pH 6. Other studies have found a similar optimal pH for phenol removal. The adsorbent surface is positively charged at pH levels less than 6, thus the sorbate and sorbent surface have minimal to no electrostatic repulsion, resulting in enhanced adsorption (Ponnuchamy et al., 2020).

Effect of initial phenol concentration

The experiment was carried out with varying initial phenol concentration (5-25 mg/L) at optimum pH of 6, at optimum biosorbent dosage of 35 g/L., and at optimum contact time of 45 min. The results show that as the phenol concentration increases, so does the adsorption capacity (Figure 7b.). However, increasing the phenol concentration decreased the efficiency percentage of phenol removal slightly (Figure 7a.). Correlating experimental data to various isotherm models will aid in understanding the interaction behavior of sorbate/sorbent.

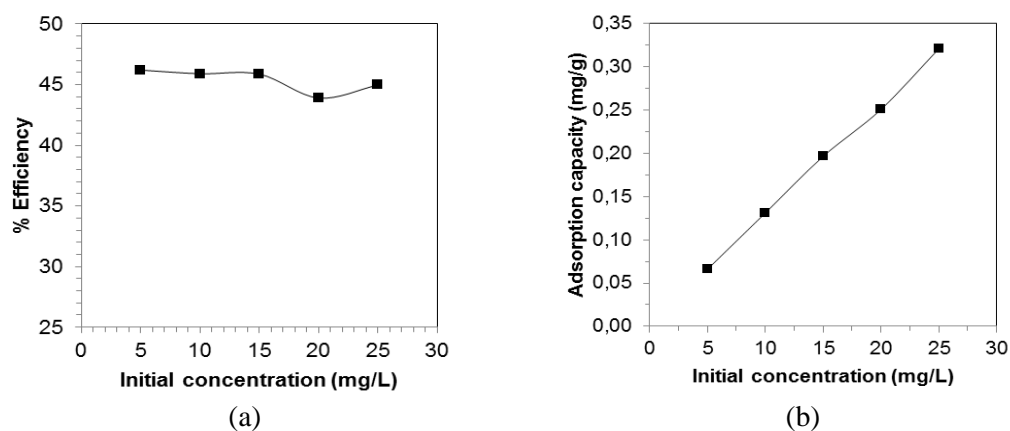


Figure 7. Efficiency percentage (a) and adsorption capacity (b) of phenol removal versus initial concentration

Study of the equilibrium isotherm

Adsorption isotherms are useful in the design of effective sorption systems in practical applications because they indicate the behavior of sorbent–sorbate interactions. In this study, several isotherm models were used to characterize the relationship between the number of phenol adsorbed and the equilibrium concentration of phenol aqueous solutions, including the Langmuir, Freundlich, Temkin, and Dubinin–Radushkevich models (Figure 8.).

The Langmuir isotherm emphasizes adsorbate monolayer chemisorption on adsorbents with identical sorption sites. Langmuir isotherm model (Langmuir, 1918) can be expressed by the equation (8) below:

$$q_e = \frac{q_m K_L C_e}{1 + K_L C_e} \quad (8)$$

The linear version of the Langmuir isotherm is provided in equation. (9)

$$\frac{1}{q_e} = \left[\frac{1}{K_L \cdot q_m} \right] \frac{1}{C_e} + \frac{1}{q_m} \quad (9)$$

where C_e (mg/L) is the equilibrium concentration of the adsorbate; The equilibrium adsorption capacity (mg/g) and the maximum adsorption capacity (mg/g) are represented by q_e and q_m respectively and K_L are Langmuir constants.

Figure 8a. shows a linear relationship of $1/q_e$ versus $1/C_e$ obtained from experimental results, indicating the applicability of the Langmuir model. The applicability of the model demands that the adsorbate is monolayer covered at the adsorbent's outer surface. Values of K_L and q_m calculated from the plot shown in Figure 8a are listed in Table 2.

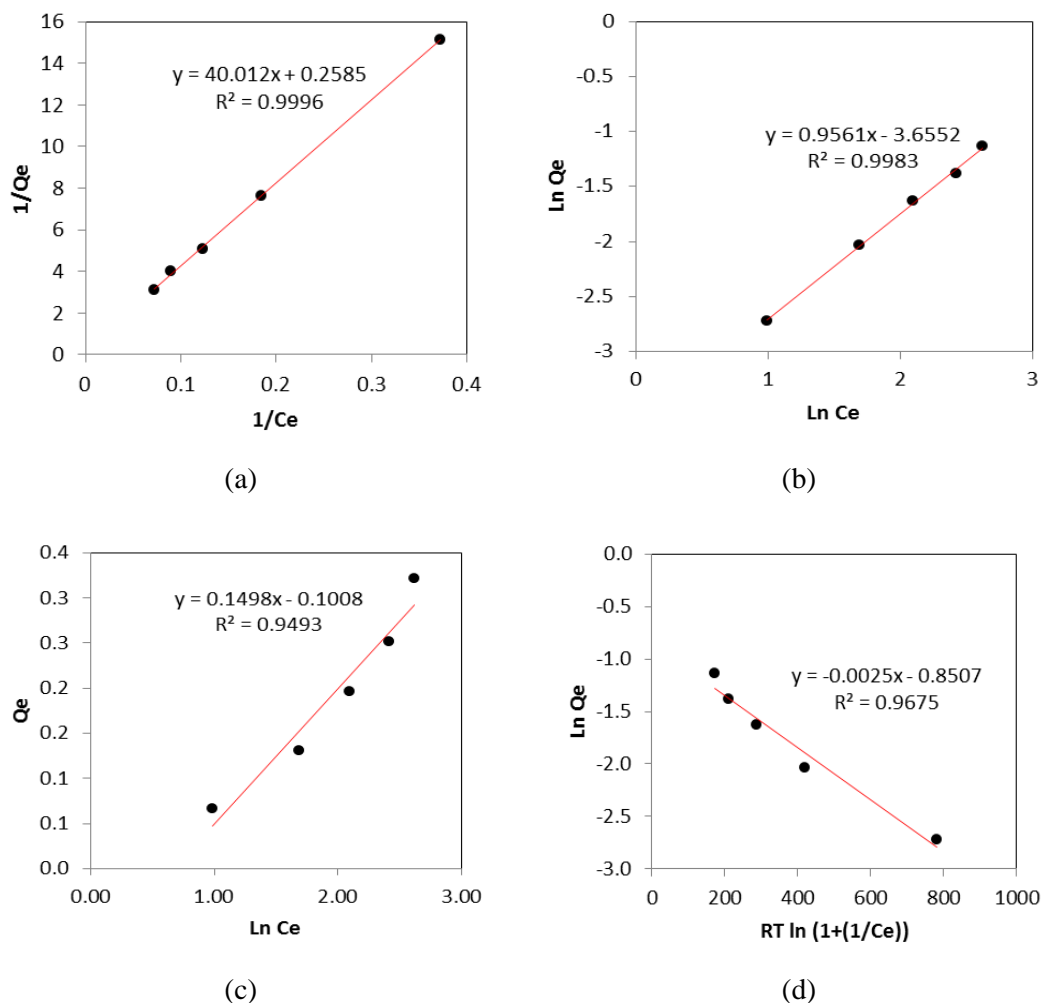


Figure 8. Adsorption isotherms applying the Langmuir model (a), the Freundlich model (b), the Temkin model (c), and the Dubinin–Radushkevich model (d)

Table 2. Calculated parameters of the adsorption isotherm models

Isotherms	Parameters
<i>Langmuir</i>	
K_L	6.436×10^{-3}
q_m (mg/g)	3.8684
R^2	0.9996
<i>Freundlich</i>	
K_F	2.585×10^{-2}
n	1.0459
R^2	0.9983
<i>Temkin</i>	
K_T	5.102×10^{-1}
B_1	0.1498
R^2	0.9675
<i>Dubinin–Radushkevich</i>	
q_d	0.4271
B_d	1.25×10^{-3}
R^2	0.9493

A non-dimensional separation factor (R_L) can be used to define the major properties of the Langmuir isotherm, which is given by:

$$R_L = \frac{1}{1 + K_L q_m} \quad (10)$$

The value of R_L specifies if the isotherm is unfavorable ($R_L > 1$), linear ($R_L = 1$), favorable ($0 < R_L < 1$), or irreversible ($R_L = 0$). The R_L value was 0.9757, indicating that, at the circumstances used in this study, the Langmuir isotherm was advantageous for phenol adsorption onto MKS.

The Freundlich model (Freundlich, 1907), which is commonly described by equation (11), describes the adsorption of adsorbates on heterogeneous surfaces.

$$q_e = K_F C_e^{\frac{1}{n}} \quad (11)$$

The Freundlich isotherm's linear form is provided in equation (12)

$$\ln q_e = \frac{1}{n} \ln C_e + \ln K_F \quad (12)$$

where K_F denotes the Freundlich equilibrium constant for adsorption capacity, and n refers for the adsorption intensity heterogeneity factor. Figure 8b. shows a linear relationship between $\ln q_e$ and $\ln C_e$. The value of n close to the limit ($0 < 1/n < 1$) indicating that the MKS surface was heterogeneous in nature.

Temkin isotherm model (Temkin & Pyzhev, 1940) is expressed in equation (13) and equation (14) represents the linear form of the Temkin isotherm.

$$q_e = \frac{RT}{b} \ln K_T C_e \quad (13)$$

$$q_e = B_1 \ln K_T + B_1 \ln C_e \quad (14)$$

where $B_1 = RT/b$. The graph (Figure 8c.) of q_e versus $\ln C_e$ calculated the Temkin constants B_1 and K_T . Values of K_T and B_1 calculated from the plot shown in Figure 8c. are listed in Table 2. To examine the impact of indirect adsorbate/adsorbate interactions on adsorption isotherms, the Temkin method was established. Because of adsorbate/adsorbate interactions, the heat of adsorption of all molecules in the layer will decrease linearly with coverage.

Another model for investigating isotherms with a good extent of rectangularity is the Dubinin–Radushkevich isotherm (Dubinin et al., 1947) analysis, that is given by equation (15) and its linear form can be represented by equation (16)

$$q_e = q_D \exp(-B_D \varepsilon^2) \quad (15)$$

$$\ln q_e = \ln q_D - 2B_D RT \ln \left(1 + \frac{1}{C_e} \right) \quad (16)$$

The $\ln q_e$ versus $RT \ln \left(1 + \frac{1}{C_e} \right)$ plot was used to get the Dubinin–Radushkevich constants, q_D and B_D values. (Figure 8d.) at 25°C are given in Table 2. Adsorption energy is then determined using ε^2 as shown in equation (17)

$$E = \frac{1}{\sqrt{2B_D}} \quad (17)$$

where E seems to be the amount of energy needed to adsorb 1 mol of phenol from its solution (kJ/mol). The process was chemical adsorption because the value of E computed here was 14.144 kJ/mol and was between 8 and 16 (Hu & Zhang, 2019).

CONCLUSIONS

The efficiency of MKS in removing phenol from its aqueous solution was investigated in this research work. It has a maximum phenol adsorption capacity of 3.86 mg/g MKS after 45

min of contact time indicating an adsorption efficiency of 46.2% for an initial concentration of 10 mg/L of phenol. The Langmuir adsorption model was also identified to be used in the adsorption process, which was verified by the Dubinin–Radushkevich isotherm equation that the process was chemically adsorbed. As a result of this study, MKS was found to be a low-cost and effective adsorbent in removing phenol from its aqueous solution. Overall, the study showed a considerable phenol removal effectiveness of MKS, which ensured its potential for further enhancement.

ACKNOWLEDGMENT

Financial support for this work from Lembaga Penelitian dan Pengabdian Masyarakat (LP2M), Universitas Nusa Bangsa.

REFERENCES

- Adewuyi, A., Gennaro, A., & Durante, C. (2015). Bioadsorbent Hura Crepitans for the removal of phenol from solution. *Journal of Water Chemistry and Technology*, 37(6), 277–282.
- Arrisujaya, D. (2014). Efisiensi Penyerapan Kulit Buah Atap (*Arenga pinnata*) Mengikat Ion-Ion Logam Kromium Dalam Larutan. *Jurnal Sains Natural*, 4(1), 58–67.
- Arrisujaya, D., Ariesta, N., & Maslahat, M. (2019). Removal of chromium (VI) from aqueous solutions using *Diospyros discolor* seed activated with nitric acid: Isotherm and kinetic studies. *Water Science and Technology: A Journal of the International Association on Water Pollution Research*, 79(6), 1214–1221.
- Dubinin, M. M., Zaverina, E. D., & Radushkevich, L. V. (1947). Sorption and structure of active carbons I. Adsorption of organic vapors. *Zhurnal Fizicheskoi Khimii*, 21, 1351–1362.
- Freundlich, H. (1907). Über die Adsorption in Lösungen. *Zeitschrift Für Physikalische Chemie*, 57U(1), 385–470.
- Haddow, G. D., Bullock, J. A., & Coppola, D. P. (2014). Natural and Technological Hazards and Risk Assessment. In *Introduction to Emergency Management* (pp. 31–70). Elsevier.
- Hameed, B. H., & Rahman, A. A. (2008). Removal of phenol from aqueous solutions by adsorption onto activated carbon prepared from biomass material. *Journal of Hazardous Materials*, 160(2–3), 576–581.
- Hevira, L., Zilfa, Rahmayeni, Ighalo, J. O., & Zein, R. (2020). Biosorption of indigo carmine from aqueous solution by *Terminalia Catappa* shell. *Journal of Environmental Chemical Engineering*, 8(5), 104290.
- Hu, Q., & Zhang, Z. (2019). Application of Dubinin–Radushkevich isotherm model at the solid/solution interface: A theoretical analysis. *Journal of Molecular Liquids*, 277, 646–648.
- Khan, Md. M. R., Sahoo, B., Mukherjee, A. K., & Naskar, A. (2019). Biosorption of acid yellow-99 using mango (*Mangifera indica*) leaf powder, an economic agricultural waste. *SN Applied Sciences*, 1(11), 1–15.
- Khraisheh, M., Al-Ghouti, M. A., & AlMomani, F. (2020). P. putida as biosorbent for the remediation of cobalt and phenol from industrial waste wastewaters. *Environmental Technology and Innovation*, 20(2020), 101148.
- Langmuir, I. (1918). The adsorption of gases on plane surfaces of glass, mica and platinum. *Journal of The American Chemical Society*, 40(9), 1361–1403.
- Legesse, M. B., & Emire, S. A. (2012). Functional and physicochemical properties of mango seed kernels and wheat flour and their blends for biscuit production. *African Journal of Food Science and Technology*, 3(9), 193–203.
- Mandal, A., Mukhopadhyay, P., & Das, S. K. (2019). The study of adsorption efficiency of rice husk ash for removal of phenol from wastewater with low initial phenol concentration. *SN Applied Sciences*, 1(2), 192.
- Moyo, M., Pakade, V. E., & Modise, S. J. (2017). Biosorption of lead(II) by chemically modified *Mangifera indica* seed shells: Adsorbent preparation, characterization and performance assessment. *Process Safety and Environmental Protection*, 111, 40–51.
- Nazaruddin, N., Arrisujaya, D., Hidayat, Zein, R., Munaf, E., & Jin, J. (2014). Batch method

- for the removal of toxic metal from water using sugar palm fruit (*Arenga pinnata* Merr) shell. *Research Journal of Pharmaceutical, Biological and Chemical Sciences*, 5(2), 1619–1629.
- Ponnuchamy, M., Kapoor, A., Pakkirisamy, B., Sivaraman, P., & Ramasamy, K. (2020). Optimization, equilibrium, kinetic and thermodynamic studies on adsorptive remediation of phenol onto natural guava leaf powder. *Environmental Science and Pollution Research*, 27, 20576–20597.
- Ramírez-García, R., Gohil, N., & Singh, V. (2019). Recent Advances, Challenges, and Opportunities in Bioremediation of Hazardous Materials. In *Phytomanagement of Polluted Sites* (pp. 517–568). Elsevier.
- Sadh, P. K., Duhan, S., & Duhan, J. S. (2018). Agro-industrial wastes and their utilization using solid state fermentation: A review. *Bioresources and Bioprocessing*, 5(1), 1.
- Sancoyo. (2018). *Kemang, Identitas Flora Kabupaten Bogor*. Pusat Konservasi Tumbuhan Kebun Raya-LIPI. <http://krbogor.lipi.go.id/id/Kemang-Identitas-Flora-Kabupaten-Bogor>
- Sharma, B., Vaish, B., Monika, Singh, U. K., Singh, P., & Singh, R. P. (2019). Recycling of Organic Wastes in Agriculture: An Environmental Perspective. *International Journal of Environmental Research*, 13(2), 409–429.
- Temkin, M. J., & Pyzhev, V. (1940). Recent modifications to Langmuir Isotherms. *Acta Physico-Chimica Sinica*, 12, 217–222.
- Zein, R., Arrisujaya, D., Hidayat, H., Elfia, M., Nazarudin, N., & Munaf, E. (2014). Sugar palm *Arenga pinnata* Merr (Magnoliophyta) fruit shell as biomaterial to remove Cr(III), Cr(VI), Cd(II) and Zn(II) from aqueous solution. *Journal of Water Supply: Research and Technology - AQUA*, 63(7), 553–559.